

# Design and Biological Evaluation of Novel, Balanced Dual PPAR $\alpha$ / $\gamma$ Agonists

Uwe Grether,<sup>\*,[a]</sup> Agnes Bénardeau,<sup>[a]</sup> Jörg Benz,<sup>[a]</sup> Alfred Binggeli,<sup>[a]</sup> Denise Blum,<sup>[a]</sup> Hans Hilpert,<sup>[a]</sup> Bernd Kuhn,<sup>[a]</sup> Hans Peter Märki,<sup>[a]</sup> Markus Meyer,<sup>[b]</sup> Peter Mohr,<sup>[a]</sup> Kurt Püntener,<sup>[a]</sup> Susanne Raab,<sup>[a]</sup> Armin Ruf,<sup>[a]</sup> and Daniel Schlatter<sup>[a]</sup>

Metabolic syndrome is diagnosed based on a cluster of clinical parameters including hyperglycemia, atherogenic dyslipidemia, central obesity and raised blood pressure. Visceral obesity, hepatic steatosis and insulin resistance have been proposed as unifying mechanisms, resulting in a prothrombotic and proinflammatory state.<sup>[1]</sup> Consequently, patients suffering from metabolic syndrome are at increased risk of progression to type 2 diabetes (T2D) and the associated micro- and macrovascular complications (e.g., coronary artery disease (CAD), stroke, renal failure, blindness and lower extremity amputation). Although improved glycemic control delays the onset of microvascular complications,<sup>[2]</sup> control of all metabolic parameters is necessary to decrease the risk of CAD.<sup>[3]</sup> Because CAD is the primary cause of mortality among patients with T2D and metabolic syndrome,<sup>[4]</sup> treatments normalizing both lipid and glucose levels have become increasingly important.

Two classes of compounds were empirically discovered decades ago, known as thiazolidinediones (TZDs) and fibrates. While the TZDs lower blood glucose as well as insulin levels and improve insulin sensitivity,<sup>[5]</sup> the fibrates are effective at lowering serum triglycerides and raising HDL cholesterol (HDL-c) levels.<sup>[6]</sup> In the past decade, the ligand-dependent transcription factors peroxisome proliferator activated receptor- $\gamma$  (PPAR $\gamma$ ) and - $\alpha$  (PPAR $\alpha$ ) have been identified as being the primary molecular targets for the antidiabetic TZDs and the lipid lowering fibrates, respectively.<sup>[7,8]</sup> This has provided new opportunities for the treatment of T2D, since the profile of a dual PPAR $\alpha$ / $\gamma$  agonist appears well suited for addressing both hyperglycemia and dyslipidemia, as well as the enhanced cardiovascular risk of diabetic patients, thereby offering a tailored therapy for T2D and its associated co-morbidities.<sup>[9,10]</sup> The pharmacological effect of agonists of the third PPAR isoform PPAR $\delta$  is less well understood but might be directed towards dyslipidemia, energy expenditure and potentially obesity<sup>[11]</sup> as well as wound healing.<sup>[12]</sup> Full PPAR $\gamma$  single agonists are linked to side effects such as edema and hemodilution.<sup>[13]</sup> Selective PPAR $\gamma$  modulators (SPPAR $\gamma$ Ms) might have the potential to overcome such problems.<sup>[14]</sup> Alternatively, PPAR $\gamma$  related side effects can be minimized by the combination of PPAR $\gamma$  potency with equal or increased potency towards PPAR $\alpha$ . In addition, such a strategy bears the potential for a combined therapy for T2D as

well as dyslipidemia and atherosclerotic progression. We therefore started a research program to identify dual PPAR $\alpha$ / $\gamma$  agonists with a PPAR $\alpha$  to  $\gamma$  affinity and potency ratio equal to or greater than one. More precisely, PPAR $\gamma$  IC<sub>50</sub> and EC<sub>50</sub> values between 0.1 and 1  $\mu$ M were envisaged to allow for sufficient potency on PPAR $\gamma$  and sufficient room to modulate PPAR $\alpha$  potency. Due to the previously described uncertainties about PPAR $\delta$  we wanted to avoid full agonism on this receptor subtype.

Information gained from studying protein–ligand X-ray co-crystal structures with PPAR ligand binding domains of all three isoforms (PPAR $\alpha$ , PPAR $\gamma$  and PPAR $\delta$ ), both from in house and from public data,<sup>[15]</sup> has provided growing insight into the factors controlling receptor binding and functional activation as well as isoform selectivity.<sup>[16–19]</sup> In all three isoforms, the ligands occupy a large, curved binding pocket adopting a common binding mode for PPAR agonists. One can schematically analyze the protein–ligand interactions of typical PPAR agonists using a simplified topological representation comprising an acidic head group, an aromatic center and a cyclic tail (Figure 1). The bifunctional acidic head group, represented so far by carboxylic acids and 2,4-thiazolidinediones, is involved in

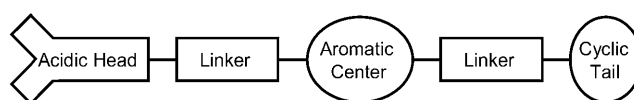


Figure 1. Simplified topological representation of typical PPAR agonists.

up to four hydrogen bonds with the receptor. This head group is crucial for PPAR activation by anchoring the flexible C-terminal transactivation helix (AF2 helix) close to the protein, thereby providing an interface together with other parts of the receptor for successful coactivator binding. The central aromatic moiety is located in a hydrophobic protein environment, while the cyclic tail region is partly solvent exposed and tolerates more polar and diverse substituents. To adapt to the curved binding site, a plethora of flexible linkers connecting the three pharmacophore features, sometimes branched to access additional subpockets, are found in known PPAR agonists. The ligand binding pockets of the three PPAR isoforms differ by several amino acids, which allow molecules to be designed that are selective for individual receptor subtypes. Capitalizing on this knowledge and guided by modeling, a set of tool compounds was synthesized from which highly promising lead compounds emerged: 1) the previously described indolyl-

[a] Dr. U. Grether, Dr. A. Bénardeau, Dr. J. Benz, A. Binggeli, D. Blum, Dr. H. Hilpert, Dr. B. Kuhn, Dr. H. P. Märki, Dr. P. Mohr, Dr. K. Püntener, Dr. S. Raab, Dr. A. Ruf, Dr. D. Schlatter  
Pharma Research, F. Hoffmann-La Roche Ltd., 4070 Basel (Switzerland)  
Fax: (+41) 61688544  
E-mail: uwe.grether@roche.com

[b] Dr. M. Meyer  
Pharma Development, F. Hoffmann-La Roche Ltd., 4070 Basel (Switzerland)

alkoxy-propionic acids,<sup>[20]</sup> and 2) simple  $\alpha$ -ethoxy-phenylpropionic acids; the latter are the subject of this communication.

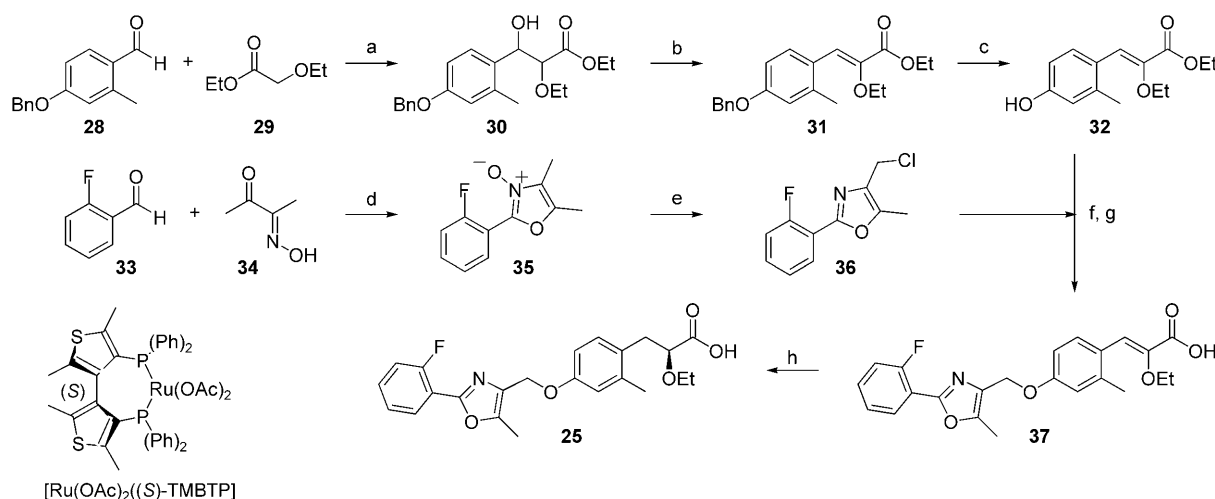
Table 1 summarizes the binding affinities and functional transactivation data of compounds investigated in this study. As indicated by the binding and functional values for compound 1, 2 and 3, the first derivatives synthesized,  $\alpha$ -ethoxy-phenylpropionic acids exhibit good intrinsic selectivity over PPAR $\delta$ . The phenyloxazole or phenylthiazole side chain, respectively, provides the desired potency towards PPAR $\alpha$  and  $\gamma$ . With respect to the alkoxy substituent in  $\alpha$  position, ethoxy is most favorable for potent dual  $\alpha$  and  $\gamma$  agonism. To assess which is the more active enantiomer both antipodes of compound 1 were synthesized (compounds 4 and 5). As described for other PPAR agonists,<sup>[20]</sup> essentially all PPAR activity can be attributed to the (S) enantiomer (4 vs 5). Due to multiple residue differences in the linker and tail region, the chain length has a significant influence on the subtype selectivity. With a

methylene linker ( $n=1$ ) a higher affinity to the  $\alpha$  receptor was observed whereas a propyl linker ( $n=3$ ) led to increased affinity towards PPAR $\gamma$  and a less pronounced increase in PPAR $\alpha$  activity (2 vs 6). Compound 1, with an ethylene linker ( $n=2$ ), shows only weak activity towards PPAR $\alpha$ . Since the methylene linker provides the desired  $\gamma/\alpha$  ratio of approximately one or higher (i.e., 3,  $\gamma/\alpha$  IC<sub>50</sub> ratio=4.2), we focused on methylene bridged compounds and introduced substituents on the terminal phenyl ring. Substitution at the 2 position leads to a decrease in  $\gamma$  affinity (2 vs 7–9). The bigger the size of the substituent the greater the loss in binding affinity; the 2-isopropoxy substituted analogue ( $R^4=2\text{-O}i\text{Pr}$ ) of compound 2 shows a PPAR $\gamma$  IC<sub>50</sub> value  $>10\text{ }\mu\text{M}$  (data not shown). In contrast, affinity and functional activity on the  $\alpha$ -receptor subtype is influenced to a much smaller extent. Substitution at the 3 position leads to potent dual PPAR $\alpha/\gamma$  agonists with a higher affinity for the  $\alpha$  receptor, for example, in the case of 3-trifluoromethyl

**Table 1.** Binding affinities and functional transactivation data of  $\alpha$ -ethoxy-phenylpropionic acids on human PPAR.<sup>[a]</sup>

Table 1. Binding affinities and functional transduction data of various phenylpropanoic acids at human PPAR $\alpha$															
Compd <sup>[c]</sup>	C-2	R <sup>1</sup>	R <sup>2</sup>	R <sup>3</sup>	R <sup>4</sup>	X	Y	n	Chemical structure			Ratio $\gamma/\alpha$	EC <sub>50</sub> [ $\mu$ M] (% Effect) <sup>[b]</sup>		
									IC <sub>50</sub> [ $\mu$ M]				$\alpha$	$\gamma$	$\delta$
									$\alpha$	$\gamma$	$\delta$				
1	rac	Me	H	Me	H	N	O	2	3.2	0.004	–	0.001	0.55 (98)	0.03 (57)	2.54 (27)
2	rac	Me	H	Me	H	N	O	1	0.23	0.46	5.89	2.0	0.07 (123)	0.06 (71)	2.22 (20)
3	rac	Me	H	H	4-Cl	N	S	1	0.11	0.46	3.57	4.2	0.08 (97)	0.61 (100)	2.61 (22)
4	(S)	Me	H	Me	H	N	O	2	0.03	0.002	–	0.06	0.04 (125)	0.01 (61)	1.80 (35)
5	(R)	Me	H	Me	H	N	O	2	> 10	0.52	–	< 0.05	2.60 (27)	1.40 (43)	> 10
6	rac	Me	H	Me	H	N	O	3	0.13	0.03	–	0.3	0.15 (94)	0.06 (104)	2.66 (16)
7	rac	Me	H	Me	2-F	N	O	1	0.12	0.65	–	5.2	0.14 (92)	0.20 (125)	2.54 (28)
8	rac	Me	H	Me	2-Me	N	O	1	0.31	0.89	–	2.9	0.18 (103)	0.95 (81)	2.51 (18)
9	rac	Me	H	Me	2-Cl	N	O	1	0.51	1.09	–	2.1	0.12 (118)	0.37 (120)	2.77 (18)
10	rac	Me	H	Me	3-Cl	N	O	1	0.24	0.07	–	0.3	0.05 (126)	0.031 (82)	2.34 (42)
11	rac	Me	H	Me	3-CF <sub>3</sub>	N	O	1	0.07	0.32	3.84	4.3	0.01 (90)	0.01 (53)	1.03 (34)
12	rac	Me	H	Me	4-O <i>i</i> Pr	N	O	1	0.18	0.11	–	0.6	0.60 (132)	0.37 (143)	2.65 (7)
13	rac	Me	H	Me	4- <i>i</i> Pr	N	O	1	0.07	0.07	1.10	1.0	0.02 (95)	0.03 (110)	1.7 (93)
14	rac	Me	H	Me	4-Cl	N	O	1	0.16	0.72	1.65	4.4	0.12 (109)	0.18 (64)	1.62 (174)
15	rac	Me	H	Me	3-Me, 4-F	N	O	1	0.17	0.32	–	1.9	0.02 (105)	0.15 (92)	2.43 (33)
16	rac	Me	H	Me	4-Cl	N	S	1	–	2.30	–	–	0.04 (210)	0.81 (58)	2.30 (20)
17	rac	Me	H	Me	4-Cl	S	N	1	0.30	1.17	0.17	3.9	0.47 (144)	0.63 (59)	3.31 (85)
18	(S)	Me	H	Me	H	N	O	1	0.08	0.31	3.78	3.8	0.11 (169)	0.08 (87)	1.45 (45)
19	(S)	F	H	Me	H	N	O	1	0.14	0.20	3.50	1.4	0.13 (104)	0.20 (87)	2.40 (15)
20	(S)	Cl	H	Me	H	N	O	1	0.05	0.18	2.70	3.5	0.15 (159)	0.24 (62)	2.8 (19)
21	(S)	Me	Me	Me	H	N	O	1	1.32	1.73	> 10	1.3	0.21 (121)	0.67 (81)	2.20 (29)
22	(S)	CF <sub>3</sub>	H	Me	H	N	O	1	0.340	0.28	0.41	0.8	0.21 (189)	0.25 (104)	0.49 (163)
23	(S)	Et	H	Me	H	N	O	1	0.31	0.12	0.50	0.4	0.04 (70)	0.02 (54)	0.62 (69)
24	(S)	Me	H	H	4-Cl	N	S	1	0.02	0.74	1.31	37.0	0.03 (108)	0.21 (114)	2.46 (46)
25	(S)	Me	H	Me	2-F	N	O	1	0.190	0.38	6.98	2.0	0.06 (123)	0.12 (66)	1.23 (39)
26	(S)	Me	H	Me	2-Me	N	O	1	0.14	1.08	5.96	7.6	0.28 (101)	0.16 (79)	2.54 (20)
27	(S)	Me	H	Me	4-O <i>i</i> Pr	N	O	1	0.03	0.06	–	1.9	0.16 (97)	0.12 (107)	2.63 (18)
Rosiglitazone <sup>[d]</sup>									> 10	0.45	> 10	< 0.05	> 10	0.45 (85)	> 10
Tesaglitazar <sup>[e]</sup>									0.48	0.35	> 10	0.8	2.95 (25)	2.67 (45)	> 10
Fenofibric acid <sup>[f]</sup>									62.8	> 100	> 100	> 1.6	69.3 (11)	> 100	> 100

[a] PPAR $\alpha$ ,  $\gamma$ , and  $\delta$  radioligand binding and functional transactivation (luciferase transcriptional reporter gene) assays were performed as described in Binggeli et al.<sup>[21]</sup> the variability of the IC<sub>50</sub> determinations was on average  $\pm 10\%$ . [b] Effects are reported in relation to reference compounds whose activity was set to 100%: farglitazar<sup>[22]</sup> (GW 262570) for PPAR $\alpha$ ; edaglitazone<sup>[23]</sup> for PPAR $\gamma$ ; GW 501516<sup>[24]</sup> for PPAR $\delta$ . [c] Molecules 1, 2, 4–6, 9, 10, 12, 14 and 15 were prepared according to Binggeli et al.<sup>[21]</sup> molecules 7, 8, 11, 13, 18–23 and 25–27 were prepared according to Binggeli et al.<sup>[25]</sup> and molecules 3, 16, 17 and 24 were prepared according to Binggeli et al.<sup>[26]</sup> [d] CAS 122320-73-4. [e] CAS 251565-85-2. [f] CAS 42017-89-0.



**Scheme 1.** Enantioselective synthesis of dual PPAR $\alpha/\gamma$  agonist **25**. *Reagents and conditions:* a) LDA, THF,  $-78^\circ\text{C}$ , 45 min, then **29**,  $\text{CH}_2\text{Cl}_2$ ,  $-78^\circ\text{C}$ , 2 h; b)  $\text{H}_2\text{SO}_4$ , DMF,  $100^\circ\text{C}$ , 1 h; c)  $\text{BF}_3\cdot\text{Et}_2\text{O}$ ,  $\text{Me}_2\text{S}$ ,  $\text{CH}_2\text{Cl}_2$ , RT, 14 h, 72% (3 steps); d)  $\text{AcOH}$ ,  $\text{HCl}_{(g)}$ ,  $0^\circ\text{C}$ , 2 h to  $22^\circ\text{C}$ , 2 h; e)  $\text{POCl}_3$ ,  $\text{CHCl}_3$ , reflux, 14 h, 50% (2 steps); f)  $\text{Cs}_2\text{CO}_3$ , KI, acetone, reflux, 14 h; g)  $\text{NaOH}$ ,  $\text{H}_2\text{O}/\text{THF}/\text{MeOH}$  (1:2:1),  $22^\circ\text{C}$ , 3 h, 93% (2 steps); h)  $[\text{Ru}(\text{OAc})_2((S)\text{-TMBTP})]$ ,  $\text{H}_2$  (60 bar),  $60^\circ\text{C}$ , 16 h, 80%, 95.2% ee, (99.9% ee after recrystallization).

substitution (compound **11**). Substitution at the 4 position results in equipotent dual  $\alpha$  and  $\gamma$  agonism (compounds **12** and **13**), or in the case of the 4-chloro substituted phenyloxazole **14** to a compound with a higher affinity for the  $\alpha$  over the  $\gamma$  receptor. Comparable  $\alpha$  selectivity was also found for the 4-fluoro-3-methyl-substituted derivative **15** and 4-chloro-substituted phenylthiazole **3**. Overall, a similar structure–activity relationship with respect to the phenyl substitution pattern was found for phenylthiazoles (data not shown). Introducing a methyl substituent at position 5 of the thiazole leads to a reduction in  $\gamma$  affinity (**3** vs **16**). The same observation was made when the positions of the nitrogen and sulfur atoms were exchanged (**3** vs **17**). Methyl substitution on the methylene bridge, or replacement of the methyl substituent by an extended alkyl chain such as ethyl in position 5 of the oxazole gives triple PPAR $\alpha/\gamma/\delta$  agonists (data not shown). In order to investigate the influence of residues  $\text{R}^1$  and  $\text{R}^2$  on the PPAR receptor subtype activities, enantiopure phenyloxazoles **19–23** were synthesized and compared with the (*S*) enantiomer of compound **2** (compound **18**). While fluoro and chloro atoms are good replacements for a methyl group (**19** and **20** vs **18**), a second methyl substituent leads to a significant reduction in  $\alpha$  and  $\gamma$  affinity (cf. **21**). Trifluoromethyl and ethyl substitution decreases selectivity against PPAR $\delta$  (**22** and **23** vs **18**). With alkoxy substituents such as methoxy or ethoxy, affinity for the  $\gamma$  receptor was lost (data not shown). For further profiling, the (*S*) enantiomers of compounds **3**, **7**, **8** and **12**, which possess the desired PPAR $\alpha/\gamma$  potency ratio equal or greater to one, were synthesized as well. Their functional activity on the  $\alpha$  and  $\gamma$  receptor subtype is higher, while the  $\delta$  values were only slightly affected (**3** vs **24**, **7** vs **25**, **8** vs **26** and **12** vs **27**). Percentage activation data in Table 1 reveal that the majority of the investigated  $\alpha$ -ethoxy phenyl propionic acids behave as full agonists for both the PPAR $\alpha$  and  $\gamma$  receptors. They are up to two orders of magnitude less potent towards the PPAR $\delta$  receptor, with  $\text{EC}_{50}$  values generally  $>1\ \mu\text{M}$ . Even at micromolar

concentrations, the majority of compounds activate this receptor only weakly or not at all. 4-Chloro substituted thiazole **24** is most selective for the PPAR $\alpha$  receptor ( $\gamma/\alpha\ \text{IC}_{50}$  ratio = 37). This effect can be attributed in part to the 4-chloro substituent since a similar result was also observed in the phenyloxazole series where the 4-chloro substituted compound **14** exhibits a higher affinity for the  $\alpha$ - than for the  $\gamma$ -receptor subtype compared to the unsubstituted phenyloxazole **2** ( $\gamma/\alpha\ \text{IC}_{50}$  ratio = 4.4, **14**; vs **2**, **2**). The main driver for this effect, however, is the replacement of the oxazole by the thiazole. This is reflected in the functional values in particular, as can be seen from the  $\gamma/\alpha\ \text{EC}_{50}$  ratios for compounds **3** (7.6), **16** (20.3) and **24** (7.0).

The enantiomerically pure compounds described in Table 1 were synthesized analogously to compound **25** depicted in Scheme 1. Benzyl protected benzaldehyde **28** was subjected to an aldol reaction with ethyl ethoxyacetate **29** providing a mixture of all four stereoisomers of propionic acid ester **30**. *Z*-selective acid catalyzed water elimination and subsequent deprotection yielded phenol **32** in an overall yield of 72%. Following the method of Goto et al.,<sup>[27]</sup> butane-2,3-dione mono-oxime **34** was reacted with 2-fluorobenzaldehyde **33** furnishing oxazole *N*-oxide **35** that was subsequently treated with  $\text{POCl}_3$  to give chloromethyl oxazole **36**. Coupling of phenol **32** and oxazole **36** was most conveniently accomplished with  $\text{Cs}_2\text{CO}_3$  and KI. Hydrolysis under basic conditions provided the  $\alpha,\beta$ -unsaturated acid **37**. Asymmetric hydrogenation using the chiral ruthenium catalyst  $[\text{Ru}(\text{OAc})_2((S)\text{-TMBTP})]$ <sup>[28]</sup> delivered the final compound **25** with an enantiomeric excess of 95.2% in quantitative yield. Recrystallization gave enantiopure material in 80% yield.

To further understand the SAR of the aryl propionic acids and especially the remarkably high  $\alpha$  selectivity of thiazole **24** ( $\gamma/\alpha\ \text{IC}_{50}$  ratio = 37), we co-crystallized the ternary complex of the human PPAR $\alpha$  receptor ligand binding domain with compound **24** and a receptor coactivator SRC-1 fragment.<sup>[29]</sup> The structure was solved to a resolution of  $2.4\ \text{\AA}$  and showed a

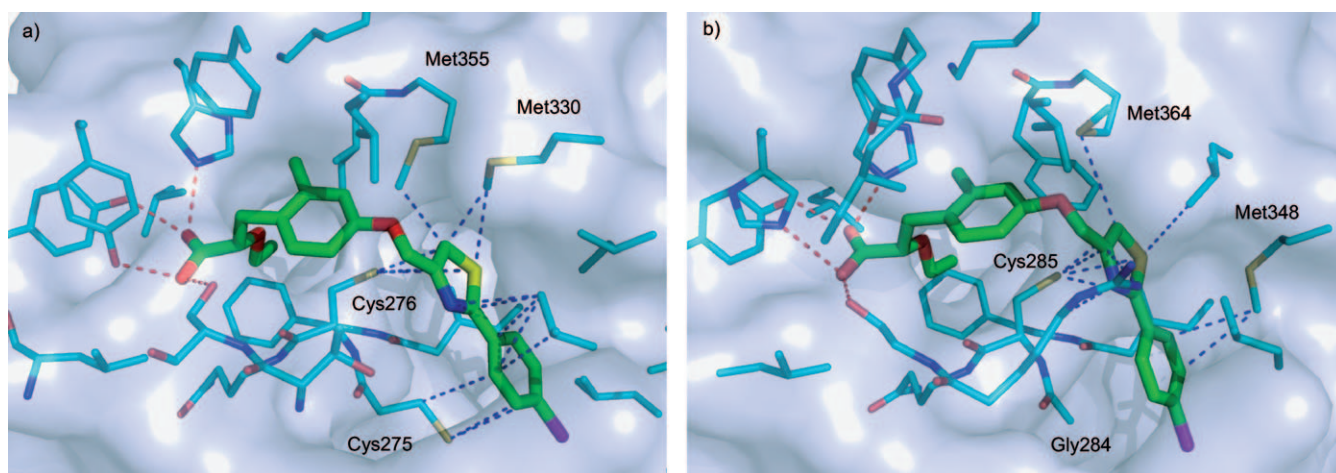


**Figure 2.** X-ray complex structures of compound **24** with a) PPAR $\alpha$  (PDB code 3FEI) and b) PPAR $\gamma$  (PDB code 3FEJ). Displayed are all protein residues with a ligand contact distance  $\leq 4.5$  Å. The four hydrogen bonds of the carboxylate head group with PPAR $\alpha/\gamma$  are shown in red. All protein contacts of the phenylthiazole tail with distances  $\leq \text{sum vdW radii} + 0.5$  Å are displayed in blue. Selected residues discussed in the text are labeled.

clear electron density for the bound ligand in the form of its (*S*) enantiomer.<sup>[30]</sup> In addition, dual agonist **24** was also co-crystallized with the ternary complex of the human PPAR $\gamma$  receptor ligand binding domain and a receptor coactivator SRC-1 fragment.<sup>[31]</sup> This structure was solved to a resolution of 2.0 Å.<sup>[32]</sup> Some residues, 259–265 for PPAR $\alpha$  and 262–274 for PPAR $\gamma$ , which are part of a flexible loop at the entrance of the binding site, showed no electron density and were not included in further considerations. The overall structure of this complex is very similar to previously published PPAR $\alpha$  and  $\gamma$  complex structures with the AF2 helix in the agonist-type conformation. Within the ligand binding sites shown in Figure 2, the typical four strong hydrogen bonds between the ligand carboxylate and the Ser, His and Tyr residues of PPAR $\alpha$  and  $\gamma$ , respectively, can be identified (all H bond distances  $\leq 3.0$  Å). Apart from the polar head group recognition, both binding sites are composed of predominantly hydrophobic side chains with limited solvent access in the central and tail region. As shown in Figure 2, a considerable number of differences in residues exist between PPAR $\alpha$  and  $\gamma$  (10 differences within 4.5 Å around the ligand **24**). While the numerous differences in residues make it challenging to associate the large  $\alpha$  selectivity of **24** with single side chain mutations, some hypotheses can be drawn from a comparison of the interactions in both isoforms. First, the overall number of interactions ( $d \leq \text{sum vdW radii} + 0.5$  Å) of the terminal phenylthiazole moiety is significantly larger in PPAR $\alpha$  (15) compared to  $\gamma$  (11). One particular difference in residues that contributes to this is Cys 275 ( $\alpha$ ) vs Gly 284 ( $\gamma$ ) yielding three additional interactions with the terminal phenyl group. Changing an oxazole into a thiazole fragment leads to a shift in the bond between the two aryl

rings and should bring the phenyl ring closer to Cys275 in PPAR $\alpha$  resulting in an increase in potency (functional activity of **14** cf. **16**). In contrast, PPAR $\gamma$  has a Gly at this position and can not profit from additional side chain–ligand interactions. Apart from the higher number of contacts, PPAR $\alpha$  also shows some interaction motifs that are particularly strong. Hydrophobic sulfur and in particular sulfur–arene interactions are known to be strongly attractive.<sup>[33]</sup> Figure 2 shows that the environment of the phenylthiazole tail is very rich in S-containing protein side chains (PPAR $\alpha$ : Cys275, Cys276, Met330, Met355; PPAR $\gamma$ : Cys285, Met348, Met364). In PPAR $\alpha$ , more hydrophobic intermolecular contacts with sulfur atoms are formed than in PPAR $\gamma$  (7 vs 6), which could further contribute to the observed isoform selectivity.

Given the desired IC<sub>50</sub>  $\gamma/\alpha$  ratios greater than one and absolute potencies ranging from PPAR $\gamma$  IC<sub>50</sub> values of 0.3–1.1  $\mu\text{M}$ , dual PPAR $\alpha/\gamma$  agonists **18**, **24**, **25** and **26** were further evaluated in more detail with respect to their physicochemical and pharmacokinetic properties (Table 2). All four compounds have a low lipophilicity with thiazole **24** possessing the highest log *D* value. This is also reflected by the somewhat lower but still reasonable thermodynamic solubility of 90  $\mu\text{g mL}^{-1}$  for this compound. Unsubstituted phenyloxazole **18** has an extremely high solubility of 2700  $\mu\text{g mL}^{-1}$ . All compounds permeate well

**Table 2.** Physicochemical and pharmacokinetic properties of compounds **18**, **24**, **25**, **26** and tesaglitazar.

Compd	Log <i>D</i> (pH 7.4) <sup>[a]</sup>	Solubility [ $\mu\text{g mL}^{-1}$ ] (pH)	PAMPA <i>P</i> <sub>eff</sub> [ $10^{-6} \text{ cm s}^{-1}$ ]	<i>F</i> (rat) <sup>[b]</sup> [%]	Cl (rat) <sup>[c]</sup> [ $\text{mL min}^{-1} \text{ kg}^{-1}$ ]	<i>V</i> <sub>ss</sub> (rat) <sup>[d]</sup> [ $\text{L kg}^{-1}$ ]	<i>t</i> <sub>1/2</sub> (rat) [h]
<b>18</b>	0.66	2700 (7.1)	5.5	53	1.86	0.6	5.6
<b>24</b>	1.57	90 (7.4)	6.5	77	0.83	0.39	6.3
<b>25</b>	0.50	434 (6.4)	3.6	95	2.25	0.68	4.3
<b>26</b>	0.89	330 (6.5)	4.3	78	2.05	1.0	7.7
Tesaglitazar	−0.05	4200 (6.0)	nd <sup>[e]</sup>	55	0.9	0.3	6.3

[a] The distribution coefficient log *D* was determined as described in reference [36]. [b] Oral bioavailability. [c] Clearance. [d] Volume of distribution. [e] Not determined.



in the parallel artificial membrane permeation assay (PAMPA).<sup>[34]</sup> Overall, all four compounds have favorable physicochemical properties, which is a prerequisite for good oral bioavailability. And indeed, these promising in vitro values translate into high oral bioavailability values (F) in rat single dose pharmacokinetic studies ranging from 53% for compound **18** up to 95% for fluoro derivative **25**. Low clearance values (Cl) and low to intermediate volumes of distribution ( $V_{ss}$ ) translate into half-life values ( $t_{1/2}$ ) ranging from 4.3 h for compound **25** up to 7.7 h for 2-methyl substituted phenyloxazole **26**, which should allow for a once daily p.o. dosing in humans. In addition to the very good physical and pharmacokinetic properties, these four compounds neither inhibit the three most important cytochrome P450 isoenzymes (3A4, 2D6 and 2C9), nor do they interact with the hERG channel, an important ion channel in the heart.<sup>[35]</sup> Finally, they did not show activity in the in vitro Ames and micronucleus test (MNT) genotoxicity assays and therefore qualified for further in vivo profiling.

Since we are aiming for a tailored therapy of T2D and associated co-morbidities like dyslipidemia, the  $\alpha$ -selective dual PPAR $\alpha/\gamma$  agonists **18**, **24**, **25** and **26** were investigated in rodent models of T2D and dyslipidemia. Initial screening for T2D was performed in db/db mice, genetically modified obese mice with a mutation in the gene coding for the leptin receptor.<sup>[37]</sup> In this model all compounds were more efficacious than the marketed pure PPAR $\gamma$  agonist rosiglitazone (data not shown).<sup>[38]</sup> In a more sophisticated euglycemic hyperinsulinemic clamp experiment, the amelioration of the insulin resistance in severely insulin-resistant Zucker fa/fa rats<sup>[39]</sup> was compared after 8 days of treatment to a fixed dose of rosiglitazone. The glucose infusion rate at steady state is a marker for insulin resistance; the higher the rate, the lower the insulin resistance. All four compounds were found to be significantly more efficacious than rosiglitazone (Table 3). Even thiazole **24**, which is the weakest with respect to affinity and functional activity on the PPAR $\gamma$  receptor—the key driver for antidiabetic efficacy—allowed for a 100-fold lower dose compared to rosiglitazone to achieve the same beneficial effects of improved insulin sensitivity. Furthermore, compounds **18**, **24** and **25** were found to be at least threefold more efficacious than the dual PPAR $\alpha/\gamma$  agonist tesaglitazar.

To assess the potential of dual PPAR $\alpha/\gamma$  agonists **18**, **24**, **25** and **26** with respect to their potential for improving the blood lipid profile, initial tests in human ApoAI mice, a transgenic animal model of dyslipidemia, have been performed.<sup>[40]</sup> After 12 days p.o. treatment at a dose of only 3 mg kg<sup>-1</sup> d<sup>-1</sup>, all four compounds showed a statistically significant improvement of blood lipid parameters, for example, they lowered blood triglyceride (TG) levels and increased HDL-c as well as apolipoprotein

**Table 3.** Equi-effective doses compared to 3.0 mg kg<sup>-1</sup> d<sup>-1</sup> p.o. of the marketed pure PPAR $\gamma$  agonist rosiglitazone.<sup>[a]</sup>

Compd	Equi-effective dose [mg kg <sup>-1</sup> d <sup>-1</sup> ] <sup>[a]</sup>
<b>18</b>	0.005
<b>24</b>	0.03
<b>25</b>	0.02
<b>26</b>	0.1
Tesaglitazar	0.1

[a] Comparison based on fa/fa rat euglycemic hyperinsulinemic clamp studies after 8 days p.o. compound treatment. [b] Comparison of glucose infusion rates at steady state and concomitant infusion of 10 mU of insulin kg<sup>-1</sup> min<sup>-1</sup> (performed in fasting state at the end of the experiment).

tein AI (apoAI) levels (data not shown). All compounds were significantly more efficacious than fenofibric acid, the active component of the clinically used PPAR $\alpha$  agonist fenofibrate;<sup>[41,42]</sup> despite the fact that the latter was administered at a much higher dose of 150 mg kg<sup>-1</sup> d<sup>-1</sup>. These lipid modulating effects were further investigated in a more elaborate dyslipidemia animal model, the high fat rat.<sup>[43]</sup> Since the majority of the lipid modulating effects are PPAR $\alpha$  driven, it is noteworthy to mention that compounds **18**, **24**, **25** and **26** dispose of similar functional activity and efficacy on human and rodent receptors (see Table 4). The same holds true for the dual PPAR $\alpha/\gamma$  agonist tesaglitazar. After 12 days p.o. treatment with phenyloxazoles **18**, **25** and **26** and phenylthiazole **24** at a dose of only 1 mg kg<sup>-1</sup> d<sup>-1</sup>, blood lipid parameters were impressively modu-

**Table 4.** Efficacy of compounds **18**, **24**, **25**, **26** and tesaglitazar on blood lipid parameters in high fat rats after 12 days p.o. treatment.<sup>[a]</sup>

Compd	human PPAR $\alpha$	EC <sub>50</sub> [ $\mu$ M] mouse PPAR $\alpha$	rat PPAR $\alpha$	TG <sup>[b]</sup>	VLDL-c <sup>[b,c]</sup>	LDL-c <sup>[b]</sup>	HDL-c <sup>[b]</sup>
<b>18</b>	0.11	0.17	0.07	-11	-31	-50	+297
<b>24</b>	0.03	0.11	0.09	-15	+11	-27	+242
<b>25</b>	0.06	0.09	0.29	-78	-47	-68	+75
<b>26</b>	0.28	0.05	0.19	-53	-18	-63	+120
Tesaglitazar	2.95	5.39	5.41	-39	-34	-50	+99

[a] 1 mg kg<sup>-1</sup> d<sup>-1</sup> dose. [b] % Change versus control. [c] Very low density lipoprotein cholesterol.

lated in a statistically significant manner. Most intriguing was the dramatic HDL-c increase, HDL-c being the most important blood lipid parameter in this experimental setting, with phenyloxazole **18** increasing HDL-c by 297% and phenylthiazole **24** by 242%, thereby reflecting the high PPAR $\alpha$  potency of the two compounds. Both compounds were found to be significantly more efficacious than tesaglitazar.

In summary, an X-ray-guided design approach has led to a novel series of  $\alpha$ -ethoxy-phenylpropionic acids being highly potent towards the PPAR $\alpha$  and  $\gamma$  receptors and showing a good selectivity against the PPAR $\delta$  receptor subtype. Side-chain variations within this series allowed the adjustment of the PPAR $\alpha/\gamma$  potency ratio ranging from equally balanced to  $\alpha$ -selective compounds. Molecules within this series possess fa-

avorable physicochemical and pharmacokinetic profiles. Phenyl-oxazoles **18**, **25**, **26** and phenylthiazole **24** show a high efficacy in animal models of T2D and dyslipidemia superior to rosiglitazone, fenofibrate and tesaglitazar. Due to their excellent overall properties including efficacy, physicochemical, pharmacokinetic and in vitro toxicological profile, these novel  $\alpha$ -ethoxy-phenyl-propionic acids qualify for further development and have a high potential for improving both glucose control (through PPAR $\gamma$  activation) and related atherogenic dyslipidemia (through PPAR $\alpha$  activation) in humans.

## Acknowledgements

The authors gratefully acknowledge contributions by Bernd Brodbeck, Caroline Brugger, Georges Hirth, Roland Humm, Dr. Michelangelo Scalone, Ernst Schaffter, Daniel Spiess and Markus Steiner to the chemical syntheses, Angele Flament and Astride Schnoebele for in vitro testing, Urs Sprecher and Philippe Verry for in vivo testing, Bernard Gsell and Martine Stihle for protein preparation and crystals, Dr. Manfred Kansy for physicochemical and Dr. Beate Bittner for in vitro toxicological and pharmacokinetic investigations.

**Keywords:** aryl propionic acids • drug design • PPAR • receptors • X-ray crystal structures

- [1] G. M. Reaven, *Diabetes* **1988**, *37*, 1595–1607.
- [2] UK Prospective Diabetes Study (UKPDS) Group, *Lancet* **1998**, *352*, 837–853.
- [3] I. M. Stratton, A. I. Adler, H. A. Neil, D. R. Matthews, S. E. Manley, C. A. Cull, D. Hadden, R. C. Turner, R. R. Holman, *Br. Med. J.* **2000**, *321*, 405–412.
- [4] D. W. Erkelens, *Am. J. Cardiol.* **2001**, *88*, 38J–42J.
- [5] T. M. Willson, P. J. Brown, D. D. Sternbach, B. R. Henke, *J. Med. Chem.* **2000**, *43*, 527–550.
- [6] J.-C. Fruchart, P. Duriez, B. Staels, *Curr. Opin. Lipidol.* **1999**, *10*, 245–257.
- [7] S. Green, *Mutat. Res.* **1995**, *333*, 101–109.
- [8] K. Schoonjans, B. Staels, J. Auwerx, *Biochim. Biophys. Acta Lipids Lipid Metab.* **1996**, *1302*, 93–109.
- [9] B. J. Goldstein, J. Rosenstock, D. Anzalone, C. Tou, K. P. Ohman, *Curr. Med. Res. Opin.* **2006**, *22*, 2575–2590.
- [10] D. M. Kendall, C. J. Rubin, P. Mohideen, J.-M. Ledezine, R. Belder, J. Gross, P. Norwood, M. O'Mahony, K. Sall, G. Sloan, A. Roberts, F. T. Fiedorek, R. A. DeFronzo, *Diabetes Care* **2006**, *29*, 1016–1023.
- [11] S. Luquet, C. Gaudel, D. Holst, J. Lopez-Soriano, C. Jehl-Pietri, A. Fredenrich, P. A. Grimaldi, *Biochim. Biophys. Acta* **2005**, *1740*, 313–317.
- [12] N. Di-Poi, L. Michalik, N. S. Tan, B. Desvergne, W. Wahli, *J. Steroid Biochem. Mol. Biol.* **2003**, *85*, 257–265.
- [13] B. R. Henke, *J. Med. Chem.* **2004**, *47*, 4118–4127.
- [14] K. Liu, R. M. Black, J. J. Acton, R. Mosley, S. Debenham, R. Abola, M. Yang, R. Tschirret-Guth, L. Colwell, C. Liu, M. Wu, C. F. Wang, K. L. MacNaul, M. E. McCann, D. E. Moller, J. P. Berger, P. T. Meinke, A. B. Jones, H. B. Wood, *Bioorg. Med. Chem. Lett.* **2005**, *15*, 2437–2440.
- [15] H. M. Berman, J. Westbrook, Z. Feng, G. Gilliland, T. N. Bhat, H. Weissig, I. N. Shindyalov, P. E. Bourne, *Nucleic Acids Res.* **2000**, *28*, 235–242.
- [16] H. E. Xu, M. H. Lambert, V. G. Montana, D. J. Parks, S. G. Blanchard, P. J. Brown, D. D. Sternbach, J. M. Lehmann, G. B. Wisely, T. M. Willson, S. A. Kliewer, M. V. Milburn, *Mol. Cell* **1999**, *3*, 397–403.
- [17] H. E. Xu, M. H. Lambert, V. G. Montana, K. D. Plunket, L. B. Moore, J. L. Collins, J. A. Oplinger, S. A. Kliewer, R. T. Gampe, Jr., D. D. McKee, J. T. Moore, T. M. Willson, *Proc. Natl. Acad. Sci. USA* **2001**, *98*, 13919–13924.
- [18] P. Cronet, J. F. W. Petersen, R. Folmer, N. Blomberg, K. Sjoblom, U. Karlsson, E. L. Lindstedt, K. Bamberg, *Structure* **2001**, *9*, 699–706.
- [19] H. E. Xu, T. B. Stanley, V. G. Montana, M. H. Lambert, B. G. Shearer, J. E. Cobb, D. D. McKee, C. M. Galardi, K. D. Plunket, R. T. Nolte, D. J. Parks, J. T. Moore, S. A. Kilewer, T. M. Willson, J. B. Stimmel, *Nature* **2002**, *415*, 813–817.
- [20] B. Kuhn, H. Hilpert, J. Benz, A. Binggeli, U. Grether, R. Humm, H. P. Maerki, M. Meyer, P. Mohr, *Bioorg. Med. Chem. Lett.* **2006**, *16*, 4016–4020.
- [21] A. Binggeli, M. Boehringer, U. Grether, H. Hilpert, H.-P. Maerki, M. Meyer, P. Mohr, F. Ricklin, (F. Hoffmann-La Roche Ltd., Basel), WO 20020506, **2002**.
- [22] L. A. Sorbera, P. A. Leeson, L. Martin, J. Castaner, *Drugs Future* **2001**, *26*, 354–363.
- [23] C. Fürsinn, B. Brunmair, M. Meyer, S. Neschen, R. Furtmüller, M. Roden, H. F. Kühnle, P. Nowotny, B. Schneider, W. Waldhäusl, *Br. J. Pharmacol.* **1999**, *128*, 1141–1148.
- [24] W. R. Oliver, Jr., J. L. Shenk, M. R. Snaith, C. S. Russell, K. D. Plunket, N. L. Bodkin, M. C. Lewis, D. A. Winegar, M. L. Sznajdman, M. H. Lambert, H. E. Xu, D. D. Sternbach, S. A. Kliewer, B. C. Hansen, T. M. Willson, *Proc. Natl. Acad. Sci. USA* **2001**, *98*, 5306–5311.
- [25] A. Binggeli, M. Boehringer, U. Grether, H. Hilpert, G. Hirth, H.-P. Maerki, M. Meyer, P. Mohr, F. Ricklin, (F. Hoffmann-La Roche Ltd., Basel), WO 2004031162, **2004**.
- [26] A. Binggeli, U. Grether, H. Hilpert, G. Hirth, H.-P. Maerki, M. Meyer, P. Mohr, (F. Hoffmann-La Roche Ltd., Basel), WO 2004020420, **2004**.
- [27] Y. Goto, M. Yamazaki, M. Hamana, *Chem. Pharm. Bull.* **1971**, *19*, 2050.
- [28] K. Puentener, M. Scalone, (F. Hoffmann-La Roche Ltd., Basel), US 2005070714, **2005**.
- [29] Co-crystals of PPAR $\alpha$  LBD with **24** were obtained using an identical protocol as described in E. Burgermeister et al. *Mol. Endocrinol.* **2006**, *20*, 809–830. Data have been collected in house on a rotating anode ( $\lambda = 1.5418$  Å) to a maximum resolution of 2.4 Å. Crystals belong to the orthorhombic space group P212121 with cell axes  $a = 42.5$ ,  $b = 75.7$ ,  $c = 97.9$  Å. For structure determination, the data have been refined against an existing in-house PPAR $\alpha$  LBD structure. Difference electron density was used to place the ligand by real space refinement.
- [30] The coordinates of the PPAR $\alpha$ -**24** co-crystal structure were deposited in the Protein Data Bank (PDB code 3FEI).
- [31] Co-crystals of PPAR $\gamma$  LBD with **24** were obtained using an identical protocol as described in E. Burgermeister et al. *Mol. Endocrinol.* **2006**, *20*, 809–830. Data have been collected in house on a rotating anode ( $\lambda = 1.5418$  Å) to a maximum resolution of 2.0 Å. Crystals belong to the orthorhombic space group P212121 with cell axes  $a = 54.2$ ,  $b = 68.8$ ,  $c = 88.8$  Å. For structure determination, the data have been refined against an existing in-house PPAR $\gamma$  LBD structure. Difference electron density was used to place the ligand by real space refinement.
- [32] The coordinates of the PPAR $\gamma$ -**24** co-crystal structure were deposited in the Protein Data Bank (PDB code 3FEJ).
- [33] E. A. Meyer, R. K. Castellano, F. Diederich, *Angew. Chem.* **2003**, *115*, 1244–1287; *Angew. Chem. Int. Ed.* **2003**, *42*, 1210–1250.
- [34] A. Avdeef, S. Bendels, L. Di, B. Fallor, M. Kansy, K. Sugano, Y. Yamauchi, *J. Pharm. Sci.* **2007**, *96*, 2893–2909.
- [35] M. C. Sanguinetti, M. Tristani-Firouzi, *Nature* **2006**, *440*, 463–469.
- [36] S. Bendels, M. Kansy, B. Wagner, J. Huwyler, *Eur. J. Med. Chem.* **2008**, *43*, 1581–1592.
- [37] R. W. Tuman, R. J. Doisy, *Diabetologia* **1977**, *13*, 7–11.
- [38] T. M. Willson, J. E. Cobb, D. J. Cowan, R. W. Wiethe, I. D. Correa, S. R. Prakash, K. D. Beck, L. B. Moore, S. A. Kliewer, J. M. Lehmann, *J. Med. Chem.* **1996**, *39*, 665–668.
- [39] V. Godbole, D. A. York, *Diabetologia* **1978**, *14*, 191–197.
- [40] E. M. Rubin, B. Y. Ishida, S. M. Clift, R. M. Krauss, *Proc. Natl. Acad. Sci. USA* **1991**, *88*, 434–438.
- [41] Fenofibrate, 1-Methylethyl 2-[4-(4-chlorobenzoyl) phenoxy]-2-methylpropanoate, CAS [49562-28-9].
- [42] The FIELD Study Investigators, *Lancet* **2005**, *366*, 1849–1861.
- [43] R. Chakrabarti, R. K. Vikramadithyan, P. Misra, J. Hiriyan, S. Raichur, R. K. Damarla, C. Gershome, J. Suresh, R. Rajagopalan, *Br. J. Pharmacol.* **2003**, *140*, 527–537.

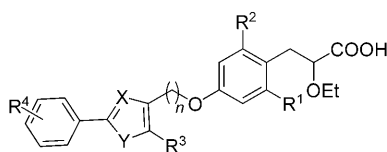
Received: December 11, 2008

Revised: February 9, 2009

Published online on ■■■■, 2009

## COMMUNICATIONS

An X-ray-guided design approach led to the identification of a novel, balanced class of  $\alpha$ -ethoxy-phenylpropionic acid-derived dual PPAR $\alpha$ / $\gamma$  agonists. The series shows a wide range of PPAR $\alpha$ / $\gamma$  ratios within a rather narrow structural space. Advanced compounds possess favorable physicochemical and pharmacokinetic profiles and show a high efficacy in T2D and dyslipidemia animal models.



U. Grether,\* A. Bénardeau, J. Benz,  
A. Binggeli, D. Blum, H. Hilpert, B. Kuhn,  
H. P. Märki, M. Meyer, P. Mohr,  
K. Püntener, S. Raab, A. Ruf, D. Schlatter

■■ – ■■

**Design and Biological Evaluation of  
Novel, Balanced Dual PPAR $\alpha$ / $\gamma$   
Agonists**